HHS Public Access

Author manuscript

Mol Cancer Res. Author manuscript; available in PMC 2018 June 01.

Published in final edited form as:

Mol Cancer Res. 2017 June ; 15(6): 765–775. doi:10.1158/1541-7786.MCR-16-0183.

INPP4B and PTEN Loss Leads to PI-3,4-P2 Accumulation and Inhibition of PI3K in TNBC

Darien E. Reed[1,2] and **Kevan M. Shokat**[1,2,*]

[1]Department of Cellular and Molecular Pharmacology, University of California, San Francisco, CA 94158

[2]Howard Hughes Medical Institute, University of California, San Francisco, CA 94158

Abstract

Triple-negative breast cancer [TNBC, lacks expression of estrogen receptor (ER), progesterone receptor (PR) and amplification of HER2/Neu] remains one of the most aggressive subtypes, affects the youngest patients and still lacks an effective targeted therapy(1,2). Both phosphatidylinositol-3-kinase (PI3K)-α and -β contribute to oncogenesis of solid tumors, including the development of breast cancer(3). Inositol polyphosphate-4-phosphatase type II (INPP4B) catalyzes the removal of the 4′-phosphate of phosphatidylinositol-(3,4)-bisphosphate (PI-3,4-P2) creating phosphatidylinositol-3-phosphate(4). There is debate concerning whether PI-3,4-P2 contributes to Akt and downstream effector activation with the known canonical signaling second messenger, phosphatidylinositol-(3,4,5)-trisphosphate (PIP3) (5–7). If PI-3,4-P2 is a positive effector, INPP4B would be a negative regulator of PI3K signaling and there is some evidence to support this(4,8). Utilizing phosphatase and tensin homolog deleted on chromosome ten (PTEN)-null triple-negative breast tumor cell lines, it was unexpectedly found that silencing INPP4B decreased basal phospho-Akt (pAkt) and cellular proliferation, and in most cases sensitized cells to PI3K-α and -β isoform-specific inhibitors. Conversely, overexpression of INPP4B desensitized cells to PI3K inhibitors in a phosphatase activity-dependent manner. In summary, the current investigation of INPP4B in PTEN-null TNBC suggests new mechanistic insight and the potential for targeted therapy for this aggressive subset of breast cancer.

Implications—These data support a model where PI-3,4-P2 is inhibitory toward PI3K, revealing a novel feedback mechanism under conditions of excessive signaling, and potentially an indication for PI3K-β isoform-specific inhibitors in PTEN-null TNBC that have lost INPP4B expression.

Keywords

Phosphatidylinositol-3; 4-bisphosphate; phosphatidylinositol-3-kinase (PI3K); Triple-negative breast cancer; Inositol polyphosphate-4-phosphatase type II (INPP4B); phosphatase and tensin homolog deleted on chromosome ten (PTEN)

*Corresponding Author: Kevan M. Shokat, University of California, San Francisco, 600 16th Street, MC2280, San Francisco, CA 94158-2280. Phone: 415-514-0472; kevan.shokat@ucsf.edu.

Conflict of Interest statement No author has a conflict of interest with the contents of this article.

Introduction

Triple-negative tumors are defined by not expressing the three known therapeutic targets, underscoring the need for new targets. The PI3K pathway is integral to cellular survival, evidenced by the cancer mutation frequencies, including 75% of breast tumors(9,10) (Supplementary Figure S1). PI3K-α and -β are Class I PI3Ks—lipid kinases that phosphorylate the D-3-hydroxyl on the inositol group of phosphatidylinositol-(4,5)-bisphosphate (PI-4,5-P_2), creating PIP_3. PTEN reverses the reaction, and is a well-established tumor suppressor protein with aberrations in all cancers including 50% of breast tumors(11,12). Loss of PTEN correlates with lack of hormone receptor (HR) expression, Triple-negative subtype and disease-related death(10,13–15). SH2 domain-containing inositol-5-phophatase 2 (Ship2) removes the 5′-phosphate of PIP_3 creating PI-3,4-P_2 and has oncogenic and tumor suppressive effects depending on cell type (16). The product of Ship2, PI-3,4-P_2, is the substrate of INPP4B, which removes the 4′ phosphate. Lower INPP4B expression in breast and ovarian tumors correlates with high tumor grade, large tumor size, lack of HR expression, co-loss of PTEN expression and poor outcome (4,8). Although all documented oncogenic driver mutations are found in *PIK3CA* (the gene encoding p110α, the catalytic subunit of PI3K-α), wild type 110β (the catalytic subunit of PI3K-β) is oncogenic when overexpressed and expression negatively correlates with HR expression while *PIK3CA* mutations positively correlate (10,14,17,18).

Small molecules targeting PI3K-β have been developed, but clinical trials have been hampered by inadequate knowledge informing patient selection(19). Preclinical studies with PI3K-β inhibitors have been inconclusive in finding markers that predict sensitivity. There is evidence that some PTEN-deficient tumors rely on PI3K-β, but attempting to correlate PI3K-β inhibitor sensitivity with *PTEN* mutational status fails to explain the range of cell line sensitivities observed (20–23). Here, we report that loss of INPP4B expression in PTEN-null Triple-negative breast cancer cell lines negatively regulates PI3K signaling and inhibits proliferation. These observations contradict the view that INPP4B is a tumor suppressor. We show that PI-3,4-P_2 accumulates with INPP4B protein loss and that resulting high levels of PI-3,4-P_2 can inhibit PI3K, decreasing PIP_3 and pAkt levels in a feedback inhibitory manner.

Materials and Methods

Cell Culture

The cell lines BT474, MCF7, MDAMB468, HCC70, BT549 and hTERT-HME1 were all purchased from the American Type Tissue Collection (ATCC, Manassas, VA) where cell lines are authenticated via short tandem repeat profiling, monitoring cell morphology, karyotyping and cytochrome C oxidase I gene species testing. All cell lines were used within 6 months of purchase and were therefore not reauthenticated. MCF7 cells were grown in DMEM Growth Medium (Life Technologies) supplemented with 10% fetal bovine serum (US-Origin Fetal Bovine Serum Heat-Inactivated, Valley Biomedical) in a 37°C 5% CO_2 incubator. BT474, HCC70 and BT549 cells were grown in RPMI 1640 Growth Medium (Life Technologies) supplemented with 10% fetal bovine serum (US-Origin Fetal Bovine Serum Heat-Inactivated, Valley Biomedical) in a 37°C 5% CO_2 incubator. MDAMB468

cells were grown in Leibovitz's L-15 Growth Medium (Life Technologies) supplemented with 10% fetal bovine serum (US-Origin Fetal Bovine Serum Heat-Inactivated, Valley Biomedical) in a 37°C 0% CO_2 incubator. hTERT-HME cells were grown in MEGM Mammary Epithelial Cell Basal Medium supplemented with the Clonetics MEGM BulletKit growth factors (BPE, hEGF, hydrocortisone and insulin; Lonza) and 1% fetal bovine serum (US-Origin Fetal Bovine Serum Heat-Inactivated, Valley Biomedical) in a 37°C 5% CO_2 incubator. Cells were passaged according to specified ATCC culture method.

Inhibitors

GDC-0941, BYL719 and AZD6482 were purchased from Selleckchem and dissolved in 100% DMSO.

Immunoblotting and Antibodies

Cells were plated into a 6-well plate at a density of 10^6 cells per well and allowed to adhere over night. The following day inhibitors were added to a final concentration of 1μM inhibitor and 0.1% DMSO. Following a one-hour incubation, cells were lysed on ice in hypotonic lysis buffer (50mM HEPES pH 7.4, 150mM NaCl); lysates were normalized for protein content by Bradford assay (absorbance at 595nm), resolved by 4–12% Bis-Tris SDS-PAGE gel (Life Technologies), transferred to nitrocellulose and blotted. All antibodies were purchased from Cell Signaling Technology (Danvers, MA) with the exception of the INPP4B antibody purchased from Abcam (Cambridge, MA) and the Ku-86 antibody purchased from Santa Cruz Biotechnology (Dallas, TX). Fluorescent secondary antibodies (800 nm emission) were purchased from LI-COR Biosciences (Lincoln, NE) and blots were visualized and bands were quantified using an Odyssey IR scanner and software (LI-COR Biosciences).

Cell Proliferation Assays

Cells were plated on a black 96-well plate with clear bottom at a density ranging from 1×10^3–5×10^3 cells per well depending on the growth rate to avoid approaching confluency over the course of the assay and allowed to adhere overnight. The following day inhibitors were added in 100 microliters (μL) of fresh growth medium at ten different final concentrations descending three-fold from 10μM. The final concentration of DMSO was 0.1% and control cells were treated with 0.1% DMSO alone. Assays at all concentrations were carried out in sextuplicate (6 repeats). The day of drug treatment, 50μL of 132μM resazurin sodium salt (Sigma Aldrich) in DPBS with calcium and magnesium (Life Technologies) was added to untreated control cells and 8 hours later the fluorescence intensity was measured using a Molecular Devices (Sunnyvale, CA) SpectraMax M5e Microplate Reader set for bottom-read fluorescence (excitation at 530 nanometers and emission at 590 nanometers). After 72 hours of treatment, resazurin was added to all wells and fluorescence intensity was measured. Data were analyzed and curves were generated using Prism 6 software.

siRNA

Cells were plated and allowed to sit for 24 hours. SMARTpool siRNA targeting INPP4B and non-targeting Control SMARTpool #4 (Dharmacon) were used with Dharmafect #1 (HCC70s and BT549s) or #4 (MDAMB468s) (Dharmafect also from Dharmacon) in OptiMEM (Life Technologies) for delivery to cells. Twenty-four hours later, medium was changed and cells were replated into 96-well plates for resazurin cell proliferation assays and 6-well plates for immunoblots.

Generation of CRISPR cell lines

A lentiviral vector containing Cas9, a cloning site for insertion of an sgRNA followed by mCherry and a puromycin resistance gene, and sgRNA sequences targeting the 5′-UTR of INPP4B were a gift from Dr. James Blau and Dr. Michael McManus, UCSF. Lentivirus was produced by the UCSF Viracore Facility and approximately 2×10^5 viral particles were added per 1×10^6 cells in one well of a 6-well plate. After 24 hours, 1 mL fresh medium was added, and another 24 hours later virus was removed and cells were replated into a 14-cm plate. Cells were allowed to sit for 24 hours and then puromycin was added at a concentration of 1 μg/mL. Medium was changed daily throughout selection. All cells died on a plate of uninfected cells treated in parallel with the same concentration of puromycin. When clones growing out reached approximately 20–30 cells, individual clones were picked and transferred to one well of a 24-well plate, removed from puromycin, expanded, and screened for INPP4B deletion by immunoblot.

Transient transfections and generation of stable cell lines

Cells were plated at a density of 2×10^6 cells per 10cm dish, allowed to sit overnight and 24 hours later FuGENE 6 Transfection Reagent from Promega (Madison, WI) was used at a ratio of 3μL reagent per 1μg DNA in OptiMEM (Life Technologies) according to manufacturer's protocol with 10μg plasmid DNA total per 10cm dish. Medium was changed 24 hours later and cells were replated into 5 wells of a 6-well plate. Cells were treated with inhibitors 24 hours later and lysates were prepared for immunoblots. For generating stable cell lines, instead of replating cells, medium was changed 24 hours post transfection and another 24 hours later fresh medium was added with 1μg/mL puromycin. Medium was changed daily, and expression was checked when cells had grown out of selection.

Phosphatidylinositol phosphate lipid extraction and ELISAs

Lipids were extracted as was described previously (24) except two 14cm plates were used per condition instead of one, and after the final extraction step, 100μL were transferred to a new glass vial for PI-4,5-P_2 measurement, 700μL were transferred to a new glass vial for PIP_3 measurement and 700μL were transferred to a new glass vial for PI-3,4-P_2 measurement. After chloroform was dried off in vacuum dryer, lipids were resuspended in 125μL PBS-Tween + 3% Protein Stabilizer (PIP_3 and PI-3,4-P_2) or 125μL PBS + 0.25% Protein Stabilizer (PI-4,5-P_2). Protein stabilizer was provided by ELISA kits (Echelon Biosciences, Salt Lake City, UT; K-3800, K-4500 and K-2500s). Each sample was analyzed in duplicate. ELISAs were carried out according to manufacturer's instructions.

Phosphatidylinositol phosphate *in vitro* lipid kinase assays

Kinase assays were carried out as described previously(25). Active PI3K-α and PI3K-β were purchased from EMD Millipore (Billerica, MA). Phosphatidylinositol phosphates were purchased from Avanti Polar Lipids (Alabaster, AL). ATP, [γ-^{32}P] was purchased from PerkinElmer (Waltham, MA). Autoradiograph was imaged using a Typhoon FLA 9000 scanner (GE Healthcare Life Sciences, Pittsburgh, PA) and image data were quantified using Spot and curves were generated using Prism 6 software.

Results

PTEN expression status fails to predict sensitivity to a PI3K-β inhibitor

To investigate genotype-drug sensitivity relationships, we treated five breast cancer cell lines covering most molecular subtypes (BT474s (Luminal B); MCF7s (Luminal A); HCC70s, BT549s and MDAMB468s (Basal-like/Triple-negative)) and immortalized mammary epithelial cells (IMEs) with three PI3K inhibitors: Pictilisib/GDC0941 (pan Class I PI3K, hereafter pan PI3Ki), Alpelisib/BYL719 (PI3K-α isoform-specific, hereafter PI3Kαi) and AZD6482 (PI3K-β isoform-specific, hereafter PI3Kβi) (1,26–31) (Figure 1 and Supplementary Figure S2). The pAkt signal at Ser473 and Thr308 (hereafter pAkt) in all lines was sensitive to the pan PI3Ki, indicating a requirement for PI3K-α and/or PI3K-β activity. The pAkt signal in the hTERT-HME1, an immortalized non-transformed human mammary epithelial cell line, and both Luminal lines (BT474 and MCF7) was sensitive to the PI3Kαi but not the PI3Kβi while the opposite was true of the Triple-negative lines (HCC70, BT549, MDAMB468) (Figure 1). Importantly, non-transformed breast cells and *PIK3CA*-mutant Luminal tumors signal through PI3K-α, but PTEN-null Triple-negative tumors apparently switch to PI3K-β. Proliferation assays were carried out to assess viability and all cell lines were sensitive to the pan PI3Ki (32). MDAMB468 and HCC70 cells were sensitive to the PI3Kβi matching the pAkt data, but BT549 cells showed little-to-no sensitivity, highlighting that lack of PTEN expression is an inconsistent marker of inhibitor sensitivity (Table 1).

Loss of INPP4B in PTEN-null Triple-negative cell lines decreases levels of pAkt and slows cell growth

Studies supporting a tumor suppressive role for INPP4B have been carried out in Luminal cell lines and non-transformed mammary epithelial cells, but clinically, INPP4B expression is frequently lost in Triple-negative tumors, often with co-loss of PTEN expression (4,8). To recreate the clinical genotype we used siRNA-mediated partial knockdown in three Triple-negative PTEN-null cell lines (HCC70, BT549 and MDAMB468). Surprisingly, silencing of INPP4B protein decreased both basal pAktS473 and pAktT308 levels, suggesting a decrease in PI3K signaling (Figures 2 and S3). BT549 cells showed the greatest INPP4B reduction and the greatest decrease in pAkt levels, while MDAMB468 cells showed the smallest reduction and the smallest decrease in pAkt levels, suggesting a correlation between INPP4B and pAkt levels (Figure 2D and S3A). To see whether the decrease in pAkt had true signaling implications and was being transmitted downstream, activation of the Akt downstream target PRAS40 was assessed by measuring pPRAS40T246 levels which indeed mirror the decreased levels of pAkt as seen in Figure 2D and quantified in Figure S3C. All

three cell lines showed GI_{50} sensitization to the PI3Kβi (Table 2 and Supplementary Figure S4). In particular, BT549 cells which were largely insensitive to the PI3Kβi (GI_{50}>3μM) became significantly more sensitive (GI_{50}<600nM) following siRNA-mediated knockdown of INPP4B, suggesting INPP4B loss may be a useful biomarker for predicting PI3Kβi sensitivity.

To further validate the effect of reduction of INPP4B protein levels, we used clustered regularly interspersed short palindromic repeat (CRISPR)-mediated gene editing (33). Two CRISPR-generated null clones were isolated from the HCC70 cell line, HCC70 CRISPR 4.3 and CRISPR 4.4 (Figure 3A). *INPP4B* loss resulted in a reduction in basal pAkt levels compared to the parental HCC70 line, corroborating the siRNA data. Additionally, pAkt levels in both HCC70 CRISPR lines showed sensitization to all inhibitors compared to the parental HCC70 line (Figure 3A–C, Supplementary Figure S5). Loss of INPP4B in the HCC70 cell line lowered the pan PI3Ki and PI3Kαi GI_{50}s with no effect on the PI3Kβi GI_{50} (Supplementary Figure S6). Both HCC70 CRISPR lines grew more slowly than the parental line in response to *INPP4B* knockout, in accordance with lower levels of pAkt but contradicting the expected result of eliminating a tumor suppressor gene (Figure 3D).

Two BT549 CRISPR clones that showed reduced but not complete loss of expression of INPP4B due to incomplete targeting of alleles were generated, BT549 CRISPR 4.2 and CRISPR 4.4. Basal pAkt levels in both CRISPR lines were lower compared to the parental BT549 line (Figure 3E–F, Supplementary Figure S7). Interestingly, the BT549 CRISPR 4.4 GI_{50} values showed greater than a five-fold sensitization to the pan PI3Ki and the PI3Kβi, and a nearly four-fold sensitization to PI3Kαi compared to the parental BT549 line (Supplementary Figure S8). The BT549 CRISPR 4.4 line grew very slowly compared to the parental line, with less BT549 CRISPR 4.4 cells alive at the end of the assay than were originally plated (Figure 3G). Therefore, loss or reduction of INPP4B expression inhibits proliferation in both the HCC70 and BT549 cell lines (Table 2). Several MDAMB468 CRISPR clones were generated, but all lines ceased growing after a few cell divisions, before protein could be isolated to assess for knockdown and INPP4B expression, again supporting a model where loss of INPP4B expression inhibits cell proliferation.

Overexpression of INPP4B in PTEN-null Triple-negative cell lines increases levels of pAkt

The finding that INPP4B knockdown sensitized PTEN-null cells to a PI3Kβi led us to ask if increased levels of INPP4B would protect PTEN-null cells from a PI3Kβi. Transient high level overexpression of INPP4B in BT549 cells increased pAkt levels and caused marked resistance to all inhibitors (Figure 4A). MDAMB468 and HCC70 cell lines either did not survive trials of several transfection reagents or survived but did not survive puromycin selection, whereas BT549 cells readily underwent successful transfection. To develop a model with lower levels of INPP4B overexpression, two mixed-population stable cell lines were generated—BT549 Flag-INPP4B-WT#1 and BT549 Flag-INPP4B-WT#2. pAkt levels were resistant to PI3K inhibitors in the INPP4B-overexpressing lines compared to the parental BT549 line (Figure 4B,F–G).

Two mixed-population stable cell lines were made expressing a catalytically dead INPP4B mutant (Cys842Ala)—BT549 Flag-INPP4B-CD#1 and BT549 Flag-INPP4B-CD#2. Despite

high levels of mutant INPP4B, there was no effect on pAkt levels (Figure 4D,F–G). These data suggest two possible models for regulation of pAkt by INPP4B. The first is that the substrate of INPP4B, PI-3,4-P_2, inhibits pAkt. The second model would be that the product of INPP4B, PI-3-P, activates the PI3K pathway. Given that PI-3-P has not been shown to stimulate Akt phosphorylation we explored whether PI-3,4-P_2 could be an inhibitor of PI3K signaling leading to a decrease in pAkt.

Following INPP4B protein loss PI-3,4-P_2 levels increase and PIP_3 levels decrease in cells

Levels of PIP_3 and PI-3,4-P_2 were measured by ELISA from BT549 cells treated with control or INPP4B siRNA, parental HCC70 cells and HCC70 CRISPR 4.3 cells (24). In BT549 and HCC70 cells PI-3,4-P_2 levels increased in response to decreasing levels of INPP4B, consistent with removing the enzyme responsible for PI-3,4-P_2 breakdown (Figure 5A). Levels of PIP_3 showed the opposite trend, with a decrease evident in BT549 and HCC70 cells when INPP4B levels were decreased. Both cell lines express Ship2 (Figure 3A, 4A), catalyzing the conversion of PIP_3 to PI-3,4-P_2. The scale of change in the lipid levels was smaller with siRNA-mediated silencing compared to CRISPR-mediated frameshift mutation. With loss of INPP4B expression, levels of PI-3,4-P_2 accumulate and levels of PIP_3 decrease, correlating with the observed decrease in pAkt levels (Figures 2 & 3). These results support an inhibitory role of PI-3,4-P_2 toward PI3K signaling. We therefore hypothesized that PI-3,4-P_2 may directly inhibit PI3K, thereby decreasing PIP_3 and pAkt levels.

High levels of PI-3,4-P_2 inhibit the kinase activity of both PI3K-α and PI3K-β

In vitro lipid vesicle kinase assays (25) were used to determine whether PI-3,4-P_2 is a PI3K inhibitor. PI3K-α and PI3K-β kinase assays with PI-4,5-P_2 substrate revealed PI3K-α was more active than and has a higher affinity for the PI-4,5-P_2 substrate than PI3K-β (Figure 5B), as previously reported (34,35). The kinase assays were repeated holding PI-4,5-P_2 constant at 80μM, above the K_m's for both enzymes, but varying the concentration of PI-3,4-P_2 or PI-3,5-P_2. The kinase activity of both PI3K-α and PI3K-β toward PI-4,5-P_2 was inhibited (at about 100μM PI-3,4-P_2 for PI3K-α and about 25μM for PI3K-β), decreasing the amount of PIP_3 created (Figure 5C). Importantly, the kinase activity of both PI3K-α and PI3K-β toward PI-4,5-P_2 was unaffected by increasing concentrations of PI-3,5-P_2 up to the maximum concentration tested of 400μM (Figure 5D). Additionally, the kinase activity of both PI3K-α and PI3K-β toward PI-4,5-P_2 was inhibited by the pan PI3K inhibitor (Figure S9). Together, these data show that PI-3,4-P_2 both accumulates in cells with INPP4B protein loss and can inhibit PI3K at high concentrations.

Discussion

We have investigated the role of INPP4B in PTEN-null Triple-negative breast cancer cell lines and found that in this setting it functions in a manner contradictory to what has been previously reported. Loss of INPP4B protein decreases levels of pAkt and sensitizes cells to PI3K inhibitors. Overexpression of INPP4B increases pAkt and makes cells resistant to PI3K inhibitors in a phosphatase-dependent manner implicating either the substrate or product phosphatidylinositol phosphate lipid in mediating this effect. We confirmed that a

decrease in INPP4B causes an increase in PI-3,4-P_2 and a decrease in PIP_3 levels. Finally, we showed that PI-3,4-P_2 can inhibit the phosphorylation of PI-4,5-P_2 and accompanying production of PIP_3 by PI3K *in vitro*. Structurally, PI-3,4-P_2 and PI-4,5-P_2 are regioisomers. One possibility is that PI-3,4-P_2 may be able to bind the PI3K active site and could therefore act as a product-like competitive inhibitor of the enzyme by blocking PI-4,5-P_2 from binding, thereby decreasing production of PIP_3. To our knowledge, this is the first documented case of a phospholipid acting as a PI3K inhibitor. Furthermore, this represents a novel feedback mechanism within the PI3K signaling pathway.

These data raise the question of why INPP4B is lost in breast (and other) cancers, particularly given the inhibitory effect on PI3K signaling and proliferation. However, it is worth noting that the proliferation assays described here were carried out on a two-dimensional plastic substrate and it would be interesting to determine in future experiments if cells would behave differently in a three-dimensional setting. The proliferation data are consistent with the observed decrease in pAkt and it is unlikely that both of these findings are artifacts of growth on a two-dimensional surface. A more likely explanation is that the cells with decreased INPP4B expression exhibit other aggressive characteristics despite growing more slowly, in accordance with previous data showing that INPP4B silencing resulted in anchorage-independent growth and dysmorphic clusters of cells in three-dimensional growth assays(4,8,36). Recently, it has been reported that both homozygous and heterozygous *Inpp4b* knockout mice have been created and neither resulted in tumors after 24 months of follow-up. When crossed with *Pten* heterozygous knockout mice, both *Inpp4b* heterozygous and homozygous compound knockout mice developed metastatic follicular-like thyroid carcinomas, but loss of *Inpp4b* did not accelerate tumorigenesis in other tissues seen with *Pten* heterozygous knockout mice(5,6). Given that these knockouts are germline mutations, it cannot be excluded that the embryos compensated by either modulating expression of Ship2 or increasing expression of another of the several 4′-phosphatidylinositol phosphate phosphatases. Additionally, if INPP4B were a tumor suppressor across all tissues, one would expect to see tumors develop in other tissues besides the thyroid.

INPP4B has been implicated in transducing a non-Akt-mediated signal via SGK3(37). We cannot rule out that this pathway might be contributing to the effects on cell growth of modulating INPP4B levels. However, because of a role of PI-3,4,5-P_3 in both the Akt-dependent and -independent pathways, it is impossible to determine the contribution of SGK3 signaling. Furthermore, studies thus far have been carried out in *PIK3CA*-mutated HR positive cell lines, which are known to have different signaling profiles than Triple-negative cell lines such as the ones used in our studies.

Further experimentation is clearly needed, but in light of these data, PI3K-β inhibitors may be clinically effective in the setting of PTEN-null and INPP4B-null Triple-negative breast cancers. Importantly, this would represent the first targeted therapy indicated for this aggressive and devastating subset of breast cancer. One hopes that this is just the first of many new insights with the potential for novel targeted therapeutics for these cancers.

Supplementary Material

Refer to Web version on PubMed Central for supplementary material.

Acknowledgments

Financial Support This work was supported by The Samuel Waxman Cancer Research Foundation and NIH R01 AI099245

The authors thank all colleagues in the laboratory for insightful discussions. The authors especially thank Dr. Flora Rutaganira for assistance with the phospholipid kinase assays and Dr. Jesse Lipp for advice with statistical analysis. The authors also thank Dr. James Blau and the McManus lab for the CRISPR lentiviral plasmid and sgRNA sequences targeting *INPP4B*. KMS thanks The Samuel Waxman Cancer Research Foundation and NIH R01 AI099245.

References

1. Sørlie T, Perou CM, Tibshirani R, Aas T, Geisler S, Johnsen H, et al. Gene expression patterns of breast carcinomas distinguish tumor subclasses with clinical implications. Proc Natl Acad Sci USA. 2001; 98:10869–74. [PubMed: 11553815]
2. Hudis CA, Gianni L. Triple-negative breast cancer: an unmet medical need. Oncologist. 2011; 16(Suppl 1):1–11.
3. Zhang H, Liu G, Dziubinski M, Yang Z, Ethier SP, Wu G. Comprehensive analysis of oncogenic effects of PIK3CA mutations in human mammary epithelial cells. Breast Cancer Res Treat. 2008; 112:217–27. [PubMed: 18074223]
4. Gewinner C, Wang ZC, Richardson A, Teruya-Feldstein J, Etemadmoghadam D, Bowtell D, et al. Evidence that inositol polyphosphate 4-phosphatase type II is a tumor suppressor that inhibits PI3K signaling. Cancer Cell. 2009; 16:115–25. [PubMed: 19647222]
5. Li Chew C, Lunardi A, Gulluni F, Ruan DT, Chen M, Salmena L, et al. In Vivo Role of INPP4B in Tumor and Metastasis Suppression through Regulation of PI3K-AKT Signaling at Endosomes. Cancer Discov. 2015; 5:740–51. [PubMed: 25883022]
6. Kofuji S, Kimura H, Nakanishi H, Nanjo H, Takasuga S, Liu H, et al. INPP4B Is a PtdIns(3,4,5)P3 Phosphatase That Can Act as a Tumor Suppressor. Cancer Discov. 2015; 5:730–9. [PubMed: 25883023]
7. Hawkins PT, Stephens LR. Emerging evidence of signalling roles for PI(3,4)P2 in Class I and II PI3K-regulated pathways. Biochem Soc Trans. 2016; 44:307–14. [PubMed: 26862220]
8. Fedele CG, Ooms LM, Ho M, Vieusseux J, O'Toole SA, Millar EK, et al. Inositol polyphosphate 4-phosphatase II regulates PI3K/Akt signaling and is lost in human basal-like breast cancers. Proc Natl Acad Sci USA. 2010; 107:22231–6. [PubMed: 21127264]
9. Baselga J. Targeting the phosphoinositide-3 (PI3) kinase pathway in breast cancer. Oncologist. 2011; 16(Suppl 1):12–9.
10. Hernandez-Aya LF, Gonzalez-Angulo AM. Targeting the phosphatidylinositol 3-kinase signaling pathway in breast cancer. Oncologist. 2011; 16:404–14. [PubMed: 21406469]
11. Yuan TL, Cantley LC. PI3K pathway alterations in cancer: variations on a theme. Oncogene. 2008; 27:5497–510. [PubMed: 18794884]
12. Chalhoub N, Baker SJ. PTEN and the PI3-kinase pathway in cancer. Annu Rev Pathol. 2009; 4:127–50. [PubMed: 18767981]
13. Depowski PL, Rosenthal SI, Ross JS. Loss of expression of the PTEN gene protein product is associated with poor outcome in breast cancer. Modern Pathology Nature Publishing Group. 2001; 14:672–6.
14. Saal LH, Holm K, Maurer M, Memeo L, Su T, Wang X, et al. PIK3CA mutations correlate with hormone receptors, node metastasis, and ERBB2, and are mutually exclusive with PTEN loss in human breast carcinoma. Cancer Res. 2005; 65:2554–9. [PubMed: 15805248]

15. Lopez-Knowles E, O'Toole SA, McNeil CM, Millar EKA, Qiu MR, Crea P, et al. PI3K pathway activation in breast cancer is associated with the basal-like phenotype and cancer-specific mortality. Int J Cancer. 2010; 126:1121–31. [PubMed: 19685490]
16. Elong Edimo W, Schurmans S, Roger PP, Erneux C. SHIP2 signaling in normal and pathological situations: Its impact on cell proliferation. Adv Biol Regul. 2014; 54:142–51. [PubMed: 24091101]
17. Carvalho S, Milanezi F, Costa JL, Amendoeira I, Schmitt F. PIKing the right isoform: the emergent role of the p110beta subunit in breast cancer. Virchows Arch. 2010; 456:235–43. [PubMed: 20130907]
18. Stemke-Hale K, Gonzalez-Angulo AM, Lluch A, Neve RM, Kuo W-L, Davies M, et al. An integrative genomic and proteomic analysis of PIK3CA, PTEN, and AKT mutations in breast cancer. Cancer Res. 2008; 68:6084–91. [PubMed: 18676830]
19. Hennessy BT, Smith DL, Ram PT, Lu Y, Mills GB. Exploiting the PI3K/AKT pathway for cancer drug discovery. Nat Rev Drug Discov. 2005; 4:988–1004. [PubMed: 16341064]
20. Ni J, Liu Q, Xie S, Carlson C, Von T, Vogel K, et al. Functional characterization of an isoform-selective inhibitor of PI3K-p110β as a potential anticancer agent. Cancer Discov. 2012; 2:425–33. [PubMed: 22588880]
21. Kang S, Denley A, Vanhaesebroeck B, Vogt PK. Oncogenic transformation induced by the p110beta, -gamma, and -delta isoforms of class I phosphoinositide 3-kinase. Proc Natl Acad Sci USA. 2006; 103:1289–94. [PubMed: 16432180]
22. Wee S, Wiederschain D, Maira S-M, Loo A, Miller C, deBeaumont R, et al. PTEN-deficient cancers depend on PIK3CB. Proc Natl Acad Sci USA. 2008; 105:13057–62. [PubMed: 18755892]
23. Barlaam B, Cosulich S, Degorce S, Fitzek M, Green S, Hancox U, et al. Discovery of a series of 8-(2,3-dihydro-1,4-benzoxazin-4-ylmethyl)-2-morpholino-4-oxo-chromene-6-carboxamides as PI3Kβ/δ inhibitors for the treatment of PTEN-deficient tumours. Bioorg Med Chem Lett. 2016; 26:2318–23. [PubMed: 26996374]
24. Costa C, Ebi H, Martini M, Beausoleil SA, Faber AC, Jakubik CT, et al. Measurement of PIP3 levels reveals an unexpected role for p110β in early adaptive responses to p110α-specific inhibitors in luminal breast cancer. Cancer Cell. 2015; 27:97–108. [PubMed: 25544637]
25. Knight ZA, Feldman ME, Balla A, Balla T, Shokat KM. A membrane capture assay for lipid kinase activity. Nat Protoc. 2007; 2:2459–66. [PubMed: 17947987]
26. Folkes AJ, Ahmadi K, Alderton WK, Alix S, Baker SJ, Box G, et al. The identification of 2-(1H-indazol-4-yl)-6-(4-methanesulfonyl-piperazin-1-ylmethyl)-4-morpholin-4-yl-thieno[3,2-d]pyrimidine (GDC-0941) as a potent, selective, orally bioavailable inhibitor of class I PI3 kinase for the treatment of cancer. J Med Chem. 2008; 51:5522–32. [PubMed: 18754654]
27. Furet P, Guagnano V, Fairhurst RA, Imbach-Weese P, Bruce I, Knapp M, et al. Discovery of NVP-BYL719 a potent and selective phosphatidylinositol-3 kinase alpha inhibitor selected for clinical evaluation. Bioorg Med Chem Lett. 2013; 23:3741–8. [PubMed: 23726034]
28. NYLANDER S, KULL B, BJÖRKMAN JA, ULVINGE JC, OAKES N, EMANUELSSON BM, et al. Human target validation of phosphoinositide 3-kinase (PI3K)β: effects on platelets and insulin sensitivity, using AZD6482 a novel PI3Kβ inhibitor. J Thromb Haemost. 2012; 10:2127–36. [PubMed: 22906130]
29. Perou CM, Sørlie T, Eisen MB, van de Rijn M, Jeffrey SS, Rees CA, et al. Molecular portraits of human breast tumours. Nature. 2000; 406:747–52. [PubMed: 10963602]
30. Subik K, Lee J-F, Baxter L, Strzepek T, Costello D, Crowley P, et al. The Expression Patterns of ER, PR, HER2, CK5/6, EGFR, Ki-67 and AR by Immunohistochemical Analysis in Breast Cancer Cell Lines. Breast Cancer (Auckl). 2010; 4:35–41. [PubMed: 20697531]
31. Kao J, Salari K, Bocanegra M, Choi Y-L, Girard L, Gandhi J, et al. Molecular profiling of breast cancer cell lines defines relevant tumor models and provides a resource for cancer gene discovery. PLoS ONE. 2009; 4:e6146. [PubMed: 19582160]
32. Atreya CE, Ducker GS, Feldman ME, Bergsland EK, Warren RS, Shokat KM. Combination of ATP-competitive mammalian target of rapamycin inhibitors with standard chemotherapy for colorectal cancer. Invest New Drugs. 2012; 30:2219–25. [PubMed: 22270257]

33. Jinek M, East A, Cheng A, Lin S, Ma E, Doudna J. RNA-programmed genome editing in human cells. Elife. 2013; 2:e00471. [PubMed: 23386978]

34. Carpenter CL, Duckworth BC, Auger KR, Cohen B, Schaffhausen BS, Cantley LC. Purification and characterization of phosphoinositide 3-kinase from rat liver. J Biol Chem. 1990; 265:19704–11. [PubMed: 2174051]

35. Yanamandra M, Kole L, Giri A, Mitra S. ATP competition of PI3K inhibitors using phosphocellulose paper approach. International Journal of Bioassays. 2014

36. Chew CL, Chen M, Pandolfi PP. Endosome and INPP4B. Oncotarget. 2016; 7:5–6. [PubMed: 26700619]

37. Gasser JA, Inuzuka H, Lau AW, Wei W, Beroukhim R, Toker A. SGK3 Mediates INPP4B-Dependent PI3K Signaling in Breast Cancer. Molecular Cell. 2014; 56:595–607. [PubMed: 25458846]

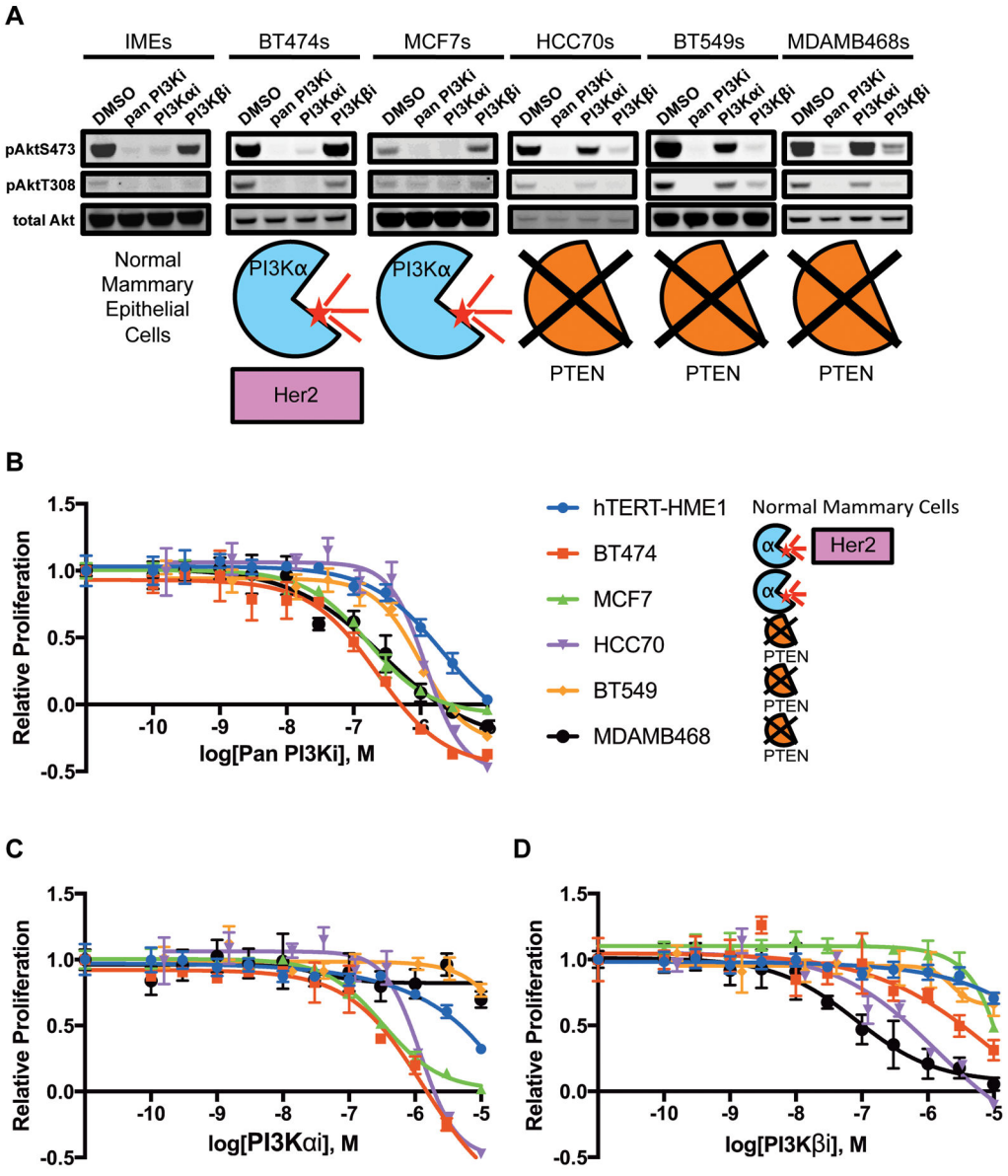

Figure 1. Breast cancer and hTERT-HME1 cell lines treated with PI3K inhibitors

A, levels of pAktS473, pAktT308 and total Akt following a 1 hour treatment with either DMSO or 1μM inhibitor (pan PI3Ki: GDC-0941, PI3K-αi: BYL719, PI3K-βi: AZD6482). B–D, kill curves generated from resazurin proliferation assays with GDC-0941 (B), BYL719 (C) and AZD6482 (D).

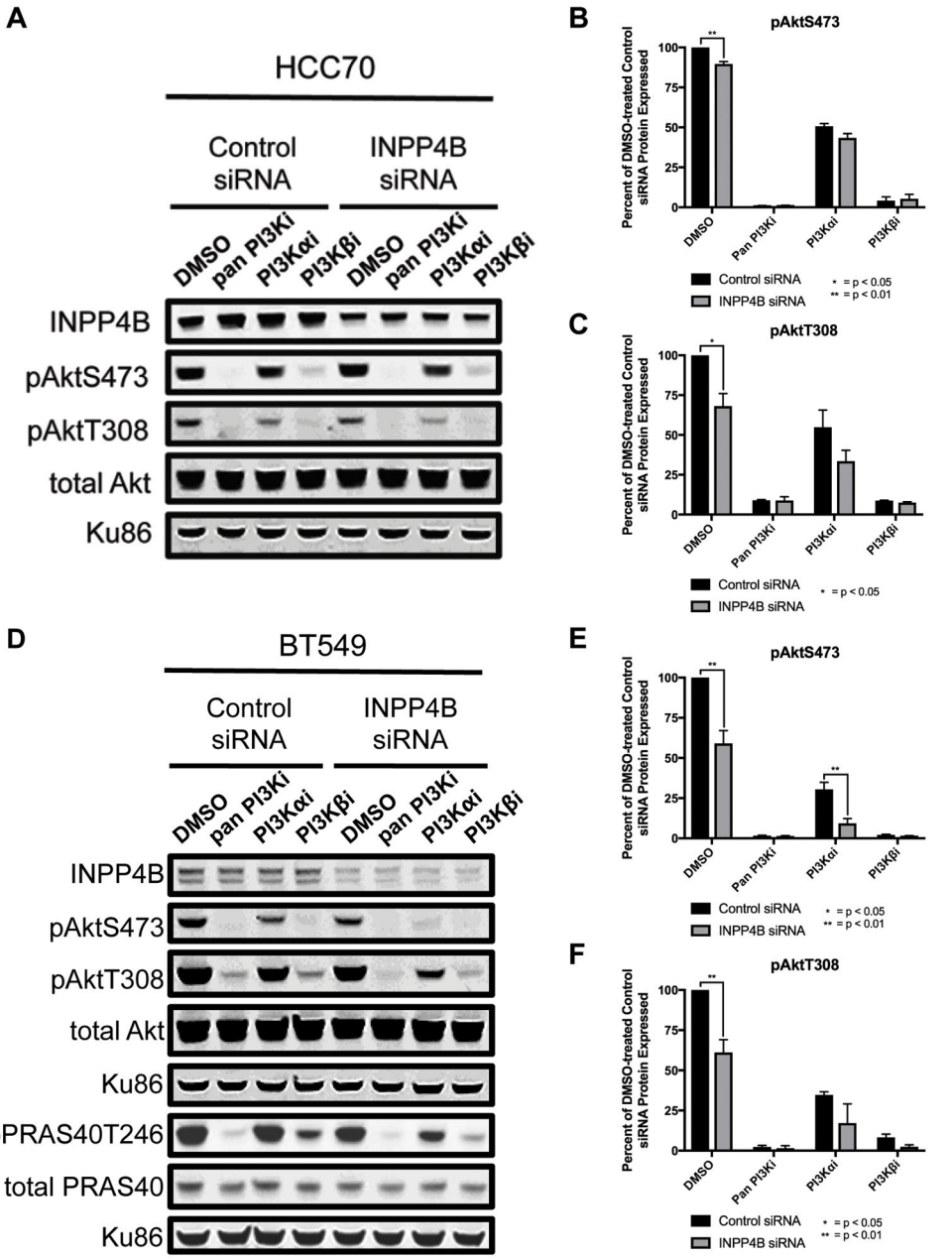

Figure 2. Effect of INPP4B siRNA on Akt signaling

A and D, HCC70 (A) and BT549 (D) cells treated with either control or INPP4B siRNA and following a 1 hour treatment with either DMSO or 1μM inhibitor; pPRAS40T246 and total PRAS40 were run on a separate blot for which the bottom Ku-86 panel is the loading control (pan PI3Ki: GDC-0941, PI3K-αi: BYL719, PI3K-βi: AZD6482). B–C and E–F, quantification of pAktS473 (B and E) and pAktT308 (C and F) signal normalized to total Akt then to the DMSO-treated control siRNA HCC70 cells (B–C) or BT549 cells (E–F), and plotted as pair-wise comparisons between control siRNA HCC70 cells and INPP4B siRNA HCC70 cells (B–C) or control siRNA BT549 cells and INPP4B siRNA BT549 cells (E–F); * and ** indicate $p<0.05$ and $p<0.01$, respectively, for unpaired one-tailed t tests between

control siRNA cells and INPP4B siRNA cells at each inhibitor concentration. Data represent the average of at least two experiments.

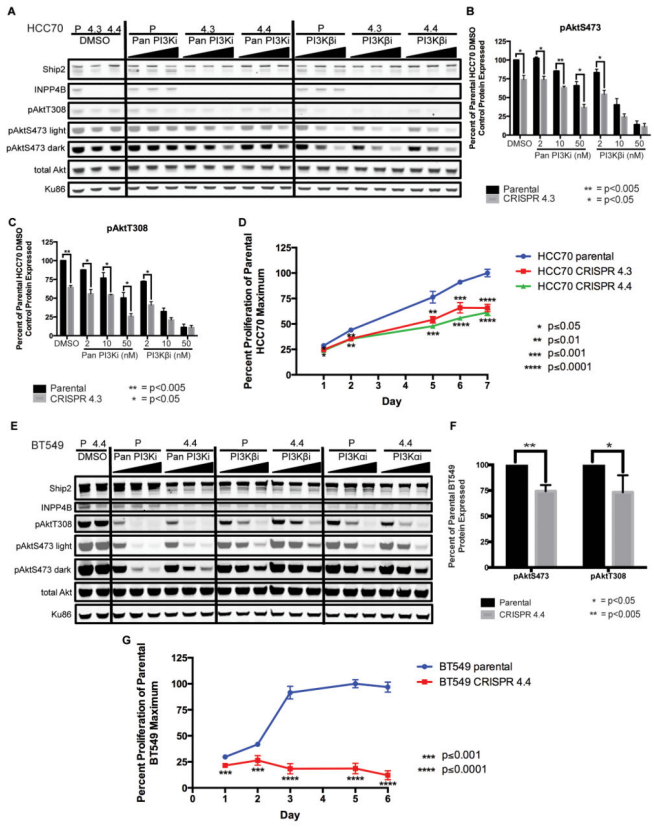

Figure 3. Effect of CRISPR-mediated knockout of INPP4B in HCC70 and BT549 cell lines on Akt signaling and rates of cell proliferation

A, parental HCC70 (P), HCC70 CRISPR 4.3 (4.3) and HCC70 CRISPR 4.4 (4.4) cells treated with DMSO, three increasing concentrations of Pan PI3Ki or three increasing doses of PI3K-βi. B–C, quantification of pAktS473 (B) and pAktT308 (C) signal normalized to total Akt then to the DMSO-treated parental HCC70 cell line, and plotted as pair-wise comparisons between parental HCC70 cells and HCC70 CRISPR 4.3 cells; * and ** indicate $p<0.05$ and $p<0.005$, respectively, for unpaired two-tailed t tests between parental HCC70 cells and HCC70 CRISPR 4.3 cells at each inhibitor concentration. Data represent the average of two experiments. D, parental HCC70, HCC70 CRISPR 4.3 and HCC70 CRISPR 4.4 cell line proliferation over 7 days, plotted as a percent of the parental HCC70 cell line maximum growth; *, **, *** and **** indicate $p\leq0.05$, $p\leq0.01$, $p\leq0.001$ and $p\leq0.0001$, respectively, for unpaired two-tailed t tests between the parental HCC70 cell line and either the HCC70 CRISPR 4.3 cell line (above red line) or the HCC70 CRISPR 4.4 cell line (below green line) on each day measurements were taken. Each day represents the mean of sextuplicate readings (six wells). E, parental BT549 (P) and BT549 CRISPR 4.4 (4.4) cells treated with DMSO, three increasing concentrations of Pan PI3Ki, three increasing doses of PI3K-βi or three increasing doses of PI3K-αi. F, quantification of pAktS473 and pAktT308 signal normalized to total Akt and then to the DMSO-treated parental BT549 cell line, plotted as pair-wise comparisons between parental BT549 cells and BT549 CRISPR 4.4 cells; * and ** indicate $p<0.05$ and $p<0.005$, respectively, for unpaired two-tailed t tests between the parental BT549 cell line and the BT549 CRISPR 4.4 cell line. Data represent

the average of two experiments. G, parental BT549 and BT549 CRISPR 4.4 cell line proliferation over 6 days, plotted as a percent of the BT549 parental cell line maximum growth; *** and **** indicate $p \leq 0.001$ and $p \leq 0.0001$, respectively, for unpaired two-tailed t tests between the parental BT549 cell line and BT549 CRISPR 4.4 cell line (below red line) on each day measurements were taken. Each day represents the mean of sextuplicate readings (six wells). (Pan PI3Ki: GDC-0941, PI3K-αi: BYL719, PI3K-βi: AZD6482; par = parental)

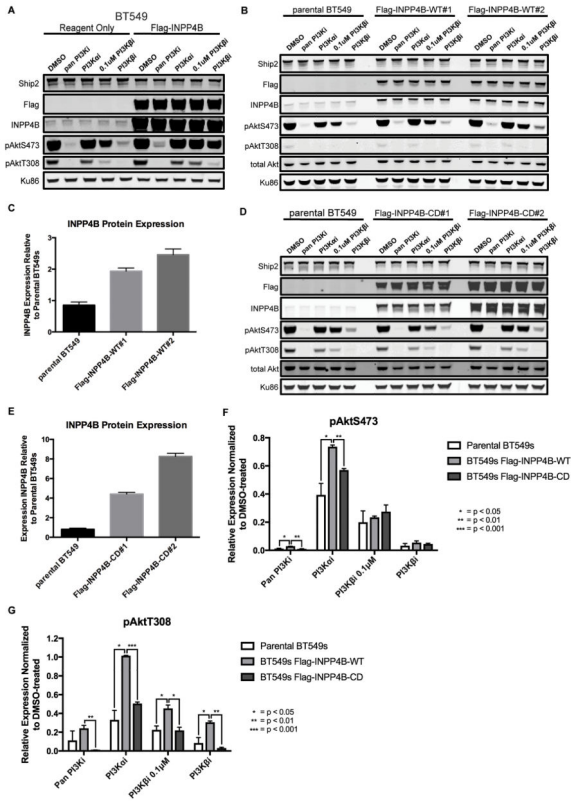

Figure 4. Effect of wild type or catalytically-dead INPP4B overexpression on pAkt levels in BT549 cells

A, BT549 cells transfected with a plasmid encoding Flag-INPP4B or reagent only, and 48 hours later treated for 1 hour with either DMSO or 1μM inhibitor except where it is noted that PI3K-βi was used at 0.1μM. Ku86 was used as a loading control. B, parental BT549, BT549 Flag-INPP4B-WT#1 or BT549 Flag-INPP4B-WT#2 cells were treated for 1 hour with either DMSO or 1μM inhibitor except where it is noted that PI3K-βi was used at 0.1μM. C, average quantified INPP4B protein expression, normalized to Ku86 loading control and then to the DMSO-treated parental BT549 cells. D, parental BT549, BT549 Flag-INPP4B-CD#1 or BT549 Flag-INPP4B-CD#2 cells were treated for 1 hour with either DMSO or 1μM inhibitor except where it is noted that PI3K-βi was used at 0.1μM. E, average quantified INPP4B protein expression, normalized to Ku86 loading control and then to DMSO-treated parental BT549 cells. F–G, quantified pAktS473 (F) and pAktT308 (G) in BT549 parental cells, Flag-INPP4B-WT cells (Flag-INPP4B-WT#1 and -WT#2 pooled) and BT549 Flag-INPP4B-CD cells (Flag-INPP4B-CD#1 and -CD#2 pooled), normalized to the DMSO-treated sample for each cell line. Cells were treated for 1 hour with either DMSO or 1μM inhibitor except where it is noted that PI3K-βi was used at 0.1μM. (pan PI3Ki: GDC-0941, PI3K-αi: BYL719, PI3K-βi: AZD6482)

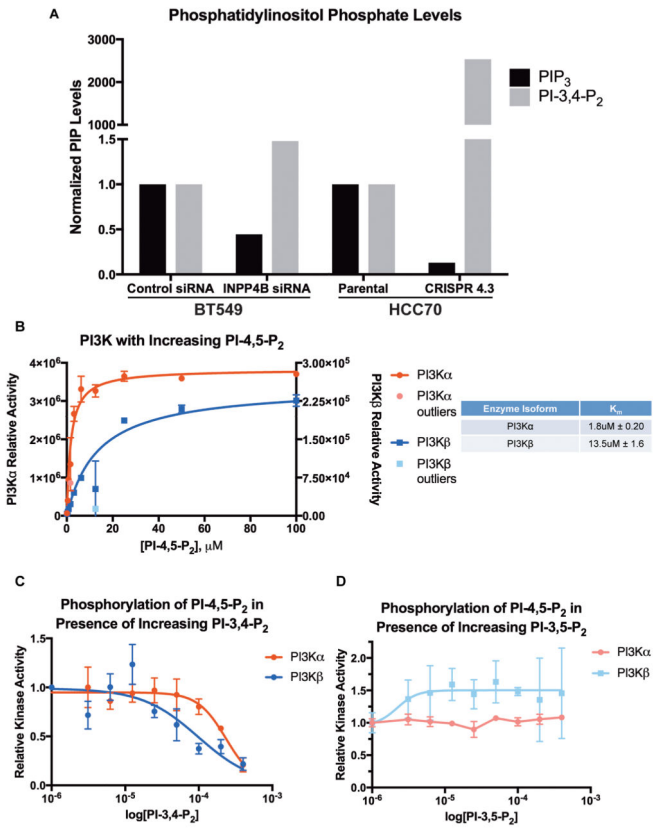

Figure 5. Cellular phosphatidylinositol phosphate levels in response to INPP4B silencing and knockout, and PI3K *in vitro* lipid kinase assays

A, BT549 cells were treated with either a non-targeting control siRNA or siRNA targeting INPP4B. Lipids were isolated and measured by ELISA; PIP_3 and PI-3,4-P_2 levels were subsequently normalized to PI-4,5-P_2 levels or to total protein. The PI-3,4-P_2 increase from undetectable in the parental HCC70 cells to 122 pmol in the HCC70 CRISPR 4.3 cells accounts for 8.5-fold more cells in the parental HCC70 cell line, but is an underestimate, as the lowest detected standard, 0.41 pmol, was used for normalization. B, PI3K-α and PI3K-β kinase activity is plotted against substrate concentration; curves and outlier calculations were generated with Prism 6 software. C, relative PI3K-α and PI3K-β kinase activity is plotted against increasing amounts of PI-3,4-P_2, with PI-4,5-P_2 substrate held constant at 80μM; data is normalized to kinase activity with no PI-3,4-P_2 and 80μM PI-4,5-P_2. Raw densitometry levels are used as a measure of kinase activity in all assays. D, relative PI3K-α and PI3K-β kinase activity is plotted against increasing amounts of PI-3,5-P_2, with PI-4,5-P_2 substrate held constant at 80μM; data is normalized to kinase activity with no PI-3,5-P_2 and 80μM PI-4,5-P_2. Raw densitometry levels are used as a measure of kinase activity in all assays.

Table 1

Mutational data and GI_{50}s for cell lines treated with PI3K inhibitors

Cell line ER, PR, HER2/Neu/ERBB2 status, *PIK3CA* mutational status, *PTEN* mutational status, other documented mutations, and inhibitor GI_{50}s observed (pan PI3Ki: GDC-0941, PI3K-αi: BYL719, PI3K-βi: AZD6482). Abbreviations: pos = positive, neg = negative, wt = wild type, mut = mutation, del = deletion, amp = amplification, missense = missense mutation, TP53 = Tumor protein p53, CDKN2A = Cyclin-dependent kinase inhibitor 2A, HDM2 = Human double minute 2 homolog, RB1 = Retinoblastoma protein, Smad4 = Mothers against decapentaplegic homolog 4 and EGFR = Epidermal growth factor receptor.

Cell Line	ER	PR	HER2	*PIK3CA*	*PTEN*	Other Mutations	Pan PI3Ki GI_{50} (μM)	PI3Kαi GI_{50} (μM)	PI3Kβi GI_{50} (μM)
IME/HMEC	pos	pos	neg	wt	wt	hTERT immortalized	1.41	4.90	>10
BT474	pos	pos	pos	K111N	wt	TP53 missense	0.09	0.30	3.31
MCF7	pos	pos	neg	E545K	wt	CDKN2A del, HDM2 amp	0.14	0.34	9.82
HCC70	neg	neg	neg	wt	nonsense mut		0.85	0.85	0.54
BT549	neg	neg	neg	wt	nonsense mut	RB1 del, TP53 missense	0.62	>10	>10
MDAMB468	neg	neg	neg	wt	nonsense mut	RB1 del, SMAD4 del, TP53 missense, EGFR amp	0.14	>10	0.10

Table 2

Comparison of PI3K inhibitor GI_{50}s for control siRNA vs INPP4B siRNA-treated cell lines and parental vs CRISPR-mediated INPP4B silencing/knockout clonal cell lines

GI_{50}s for control siRNA vs INPP4B siRNA-treated HCC70, BT549 and MDAMB468 cell lines and GI_{50}s for parental vs CRISPR-mediated INPP4B silencing/knockout HCC70 and BT549 clonal cell lines. GI_{50}s were calculated with Graphpad Prism 6.0 using proliferation assay data. (pan PI3Ki: GDC-0941, PI3K-αi: BYL719, PI3K-βi: AZD6482)

Cell Line	Knockdown Method	Condition	Pan PI3Ki GI_{50}(μM)	PI3Kαi GI_{50}(μM)	PI3Kβi GI_{50}(μM)
HCC70s	siRNA	Control	0.054	1.63	0.053
		INPP4B	0.084	0.081	0.026
	CRISPR	Parental	0.237	6.90	0.183
		INPP4B	0.093	2.56	0.296
BT549s	siRNA	Control	0.400	>10	3.41
		INPP4B	0.157	1.67	0.578
	CRISPR	Parental	0.632	>10	>10
		CRISPR	0.103	3.26	2.12
MDAMB468s	siRNA	Control	0.101	3.16	0.131
		INPP4B	0.248	>10	0.041